

Compressive-sensing-based lossy compression for hyperspectral images using spectral unmixing

Wang Zhongliang¹, Feng Wentian², Nian Yongjian³

(1. Department of Electric Engineering, Tongling University, Tongling 244061, China;

2. Branch 72 of No. 32142 Army, Baoding 071000, China;

3. School of Biomedical Engineering and Imaging Medicine, Army Medical University(Third Military Medical University),
Chongqing 400038, China)

Abstract: In the compressive sensing theory, the robust reconstruction of signals can be obtained from far fewer measurements than those obtained by the Nyquist theorem. Thus, it has a great potential in the onboard compression of hyperspectral images using minimal computational resources and storage memory. In this paper, a compressive-sensing-based hyperspectral image compression method was presented using spectral unmixing. At the encoder, the original image was compressed acquired by spatial sampling and spectral sampling, respectively. Then, the spectral and spatial correlation of the compressed data were studied. To improve the compression performance, spectral linear prediction was used to remove the spectral correlation, and the predictive errors were compressed by JPEG-LS in a lossless manner to generate the final bit-streams. At the decoder, the bit-streams were first decoded to obtain the sampled data. Then, a spectral unmixing technique was employed to reconstruct the original hyperspectral image, which can avoid the defect of conventional compressed sensing reconstruction. Experiments on data from the Airborne Visible/Infrared Imaging Spectrometer sensor show that the proposed algorithm provides better compression performance than JPEG2000 and DCT-JPEG2000 with a lower computational complexity.

Key words: hyperspectral image; compressive sensing; spectral decorrelation; spectral unmixing

CLC number: TP751 **Document code:** A **DOI:** 10.3788/IRLA201847.S126003

结合光谱解混与压缩感知的高光谱图像有损压缩

王忠良¹, 冯文田², 粘永健³

(1. 铜陵学院 电气工程学院, 安徽 铜陵 244061; 2. 32142 部队 72 分队, 河北 保定 071000;

3. 陆军军医大学(第三军医大学) 生物医学工程与影像医学系, 重庆 400038)

摘要: 压缩传感技术可以利用远少于奈奎斯特采样定理所获得的采样数据进行信号的鲁棒性重建。因此, 该技术在计算资源和存储空间均受限的高光谱图像压缩中具有很大的应用潜力。提出了一

收稿日期: 2018-03-23; 修订日期: 2018-05-19

基金项目: 安徽高校自然科学研究重点项目(KJ2016A884); 安徽省级质量工程项目(2016zy126);

重庆市基础科学与前沿技术一般项目(cstc2016jcyjA0539)

作者简介: 王忠良(1980-), 男, 副教授, 博士, 主要从事遥感图像处理方面的研究。

通讯作者: 粘永健(1982-), 男, 副教授, 博士, 主要从事遥感图像处理方面的研究。Email: yjnian@126.com

种基于压缩感知与光谱解混的高光谱图像压缩算法。在编码端,分别通过空间采样和光谱采样来实现图像采样点的压缩;然后,对采样数据的空间与谱间相关性进行了研究。为了提高压缩性能,采用谱线性预测去除采样后的谱间相关性,利用 JPEG-LS 对预测误差进行编码来生成最终的比特流。在解码端,首先解码比特流以获得采样数据;采用光谱解混技术对原始高光谱图像进行重构,克服了传统压缩感知重建的诸多不足。针对机载可见/红外成像光谱仪数据的实验结果表明,该算法比 JPEG2000 和 DCT-JPEG2000 具有更好的压缩性能,并具有较低的计算复杂度。

关键词: 高光谱图像; 压缩感知; 光谱去相关; 光谱解混

0 Introduction

Hyperspectral imaging records hundreds of spectral bands for each pixel, each of which contains values that correspond to the reflected light in a defined range of the electromagnetic spectrum. With the increase in spectral and spatial resolutions, the data volume of hyperspectral images rapidly increases. This immense data volume engenders significant challenges for onboard storage and transmission. To solve this problem, efficient compression of the hyperspectral image has received considerable attention in recent years. Recent lossy compression methods have increasingly attracted attention because lossless compression methods are unable to provide the desired compression ratio. In general, the satellite platforms have limited capacity for storage memory and computational resources; therefore, these systems usually employ a simple technique to perform data compression.

Although low-complexity KLT schemes, such as the spectral decorrelator, have been proposed^[1-3], the complexity has not been significantly reduced to an acceptable degree for hardware implementation. Moreover, transform-based algorithms always require a considerable volume of memory, as they are simultaneously performed on all spectral vectors. Meanwhile, compressive sensing (CS)^[4] is a relatively new theory for signal acquisition and reconstruction. Compared with traditional methods, this scheme can significantly reduce the consumption of imaging resources. Several hyperspectral compressive sensing

(HCS) methods have been proposed. Fowler proposed compressive-projection principal component analysis (CPPCA)^[5], which is driven by projections at the sensor onto randomly chosen lower-dimensional subspaces. Given only these random projections, the CPPCA decoder recovers not only the coefficients associated with the PCA transform but also an approximation to the PCA transform basis. Experimental results on hyperspectral data showed that CPPCA outperformed a multiple-vector variant of compressed sensing for the reconstruction quality. However, although HCS methods significantly reduce the costs of imaging, storage, and transmission, a means of precisely reconstructing the original image from a few measurements remains challenging. Jia proposed an efficient reconstruction approach for compressive sensors by exploiting four important priors: spatial piecewise smoothness, adjacent spectrum correlation, low rank, and a structure similarity property^[6]. Chen proposed multi-hypothesis prediction (MH) to exploit the spatial correlation of neighboring pixels for the compressive-projection hyperspectral image^[7]. Based on the correlation coefficients between bands, a two-phase hypothesis generation procedure was used to recover the hyperspectral image. However, the MH computational complexity was extremely high, and the algorithm was invalid when the sampling rate was less than 0.2.

Meanwhile, the hypothesis of linear mixture model (LMM) was introduced for HCS. Li compressed the hyperspectral image along the spatial domain and unmixed the hyperspectral image into a spatially

continuous abundance matrix with a given endmember matrix^[8]. Zhang compressed the hyperspectral image along the spectral domain and estimated an abundance matrix by a locally similar sparsity prior with a redundant endmember library^[9]. However, it is difficult to obtain the endmember or endmember library through this approach while collecting compressed hyperspectral data. Wang proposed a spatio-spectral hybrid compressive sensing (SSHCS) scheme based on spectral unmixing, which estimates endmembers and the corresponding abundance fraction from spatial and spectral sampled data, respectively^[10]. In Ref.[11], the hierarchical reweighted Laplace prior was proposed for reconstruction, and a latent variable-based Bayesian model was employed to learn the optimal configuration of the reweighted Laplace prior. Experimental results showed that the reweighted Laplace prior-based HCS method was adaptive to the unknown noise scene. Despite the above advancements, to the best of our knowledge, the CS technique has not been effectively used in hyperspectral images compression. In most cases, it has only been used to perform sampling and reconstruction with no encoding of the sampled data. The only work to date that applies CS in hyperspectral image compression was presented in Ref. [12], where a direct scheme that leverages the spectral correlation to compress the CS hyperspectral image was proposed. In addition, a designed flexible recovery strategy was presented to speed up the reconstruction. However, its performance was not comprehensively evaluated. In this paper, we therefore propose a CS-based lossy compression technique for hyperspectral images using spectral unmixing, whereby spatio-spectral hybrid sampling is performed on the original hyperspectral image to fully exploit its high degree of correlation. Because a strong spectral correlation continues to exist among the sampled data, spectral linear prediction is used to further remove the spectral correlation, followed by JPEG-LS lossless compression. At the decoder, spectral

unmixing is performed on the decoded image to reconstruct the original image based on a linear mixture model. Experimental results show that the proposed algorithm has competitive performance and low complexity compared to the existing transform-based algorithms.

1 Compressive-sensing-based hyperspectral image compression

Compressed sensing technology mainly involves sampling and recovering the original data. It should be noted that the CS technique only reduces the volume of original data; moreover, the dynamic range of the sampled data is much larger than that of the original data. For data storage or transmission, it is necessary to employ an efficient compression technique to encode the sampled data.

The solution of the convex l_1 -norm is widely used in CS recovery. For HCS recovery, some priors are generally introduced, such as total variation(TV), low rank, and structure similarity^[6]. However, the optimal coefficients between multiple priors are difficult to calculate, which may significantly reduce the recovery accuracy. In addition, owing to the constant iterative calculation, HCS recovery typically has a high computational complexity from using the solution of the convex l_1 -norm. In the proposed approach, the spectral unmixing is thus employed to perform the HCS recovery, which estimates endmembers and the corresponding abundance from the sampled data. It then recovers the original data based on the LMM. A flowchart of the proposed algorithm is shown in Fig.1, where the spatio-spectral hybrid sampling is performed on the original data at first to obtain the sampled data at the encoder. Then, spectral linear prediction is used to remove the spectral correlation of sampled data, followed by JPEG-LS lossless compression. At the decoder, spectral unmixing is performed on the decoded sampled data to recover the original data.

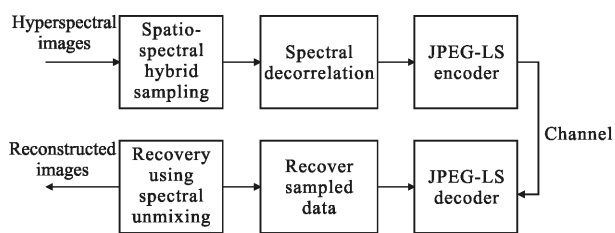


Fig.1 Flowchart of the proposed algorithm

1.1 Spatio-spectral hybrid sampling

Unlike a natural image, the hyperspectral image can be regarded as a three-dimensional data cube. To represent the hyperspectral images, we define a matrix $X=[x_1, x_2, \dots, x_L]$, where x_l ($l=1, 2, \dots, L$) is a one-dimensional vector corresponding to the l -th band (reshaped as a one-dimensional vector) with an MN length.

The spatio-spectral hybrid compressive sampling scheme is employed to perform hyperspectral CS. By using this scheme, the observation data consists of two parts, one part is the spatial compressive sampled data, $Y_1=A_1X$; the other part is the spectral compressive sampled data $Y_2=XA_2^T$, where A_1 is the spatial measurement matrix with a size of $P \times MN$, and A_2 is the spectral measurement matrix with a size of $K \times L$. By the well-known properties of the Kronecker product, ' \otimes ', the total observed data Y is composed of spatial sampled data Y_1 and spectral sampled data Y_2 , which can be converted into a standard form as:

$$Y = \begin{bmatrix} Y_1 \\ Y_2 \end{bmatrix} = AX \quad (1)$$

Complete measurement matrix A can be written as:

$$A = \begin{bmatrix} I_L \otimes A_1 \\ A_2 \otimes I_N \end{bmatrix} \quad (2)$$

where I_L and I_N denotes the identity matrix with dimensions of $L \times L$ and $N \times N$, respectively.

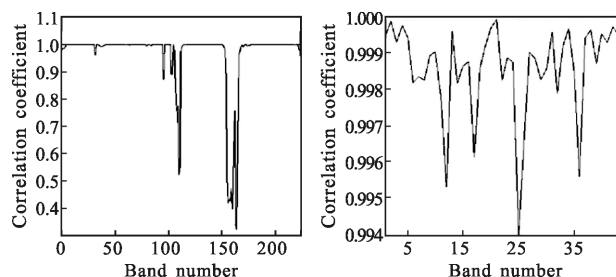
For matrix A_1 , a special kind of measurement matrix is employed, where each row of the measurement matrix contains only one "1" element, while the others are "0". Owing to the special characteristic of A_1 , the range of Y_1 is the same as X . For the spectral measurement matrix, we chose the

general random projection matrix, A_2 . Note that the total sampling rate (SR) is the sum of the spatial sampling rate, SR_1 , and the spectral sampling rate, SR_2 , where $SR_1=P/MN$ and $SR_2=K/L$.

1.2 Correlation analysis of sampled data

As noted, the hyperspectral image has both spatial and spectral correlations. To achieve high compression performance, the above correlation must be considered. For the proposed algorithm, there are two sampling approaches: spatial sampling and spectral sampling. Before the compression algorithm is used on the sampled data, it is necessary to exploit the spectral and spatial correlations of the sampled hyperspectral image.

Figure 2 (a) provides the spectral correlation of the hyperspectral image sampled by spatial sampling with $SR_1=0.01$. Figure 2 (b) presents the spectral correlation of the hyperspectral image sampled by spectral sampling with $SR_2=0.2$. As shown, a strong spectral correlation exists in the sampled hyperspectral image. Thus, to achieve high performance, an efficient algorithm should be employed to remove the spectral correlation.

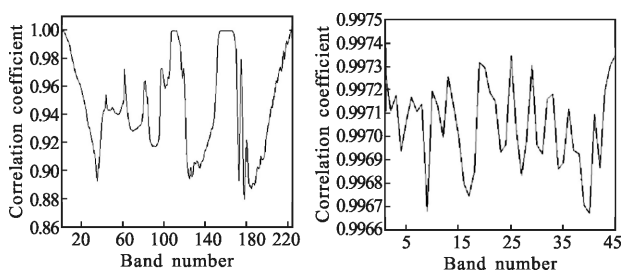


(a) Spatial sampling($SR_1=0.01$) (b) Spectral sampling ($SR_2=0.2$)

Fig.2 Spectral correlation of the sampled hyperspectral image

Figure 3 depicts the spatial correlation of each band sampled in the above two approaches. Regardless of which sampling manner is employed, it is apparent that the sampled data still has a strong spatial correlation that should be removed by an effective compression algorithm. With respect to onboard hyperspectral image compression, the sampled elements must be encoded by a certain compression

technique to be transmitted to the decoder in the ground. On the other hand, the values of the sampled elements are usually much larger than those of the original elements since each sampled element is obtained by weighting all original elements using each row of the measurement matrix. Therefore, it is necessary to compress the sampled elements to achieve real-time transmission with limited bandwidth for the onboard hyperspectral image.



(a) Spatial sampling($SR_1=0.01$) (b) Spectral sampling($SR_2=0.2$)

Fig.3 Spatial correlation of the sampled hyperspectral image

1.3 Prediction-based compression for sampled data

Information loss occurs in HCS; thus, to ensure the reconstructed quality, lossless compression is selected to encode the sampled data. In particular, linear prediction is employed to remove the spectral correlation since the prediction-based algorithm can provide perfect performance for lossless compression with low complexity.

For the hyperspectral image obtained by spectral sampling, each band is divided into non-overlapping blocks with a size of $s \times s$ for adaptation to the local features. Let $x_{k,i,j}$ denote the pixel of the current block in the i -th line, j -th pixel, and k -th band, with $k=1,2,\dots,K$ and $i,j=1,2,\dots,s$. The pixel $x_{k,i,j}$ is linearly predicted from the decoded pixels $x_{k-1,i,j}$ of the previous block. Let μ_k be the average value of the current block and let μ_{k-1} be the average value of the co-located block in the $(k-1)$ -th band. The predicted value of the current block can be expressed as:

$$\bar{x}_{k,i,j} = \alpha_k(x_{k-1,i,j} - \mu_{k-1}) + \mu_k \quad (3)$$

where α_k is the prediction coefficient, which can be computed by the least-squares estimator as:

$$\alpha_k = \frac{\sum_{i=1}^N \sum_{j=1}^N (x_{k-1,i,j} - \mu_{k-1})(x_{k,i,j} - \mu_k)}{\sum_{i=1}^N \sum_{j=1}^N (x_{k,i,j} - \mu_k)(x_{k,i,j} - \mu_k)} \quad (4)$$

The predictive error can be calculated as:

$$e_{k,i,j} = x_{k,i,j} - \bar{x}_{k,i,j} \quad (5)$$

The error samples of each block are compressed in a lossless manner by JPEG-LS to generate the final bit-stream because JPEG-LS can effectively remove the spatial correlation of each block and achieve better lossless compression performance.

2 Recovery of the hyperspectral images

At the decoder, we can easily obtain the sampled data by using JPEG-LS and inverse spectral linear prediction. For CS recovery, the application of matrix decomposition has been proven as an effective technique^[5]. In this paper, we employ spectral unmixing to reconstruct original data from the compressive sampled data. It is known that the hyperspectral image is usually regarded as a linear mixture model (LMM) for spectral unmixing. Based on LMM, hyperspectral images X can be written as:

$$X = \sum_{i=1}^p s_i e_i = SE \quad (6)$$

where the matrix $X = [x_1, x_2, \dots, x_L]$ represents the hyperspectral images, and the endmember matrix $E = [e_1, e_2, \dots, e_p]^T$ is a $p \times L$ matrix consisting of p endmember signatures, and abundance matrix $S = [s_1, s_2, \dots, s_p]^T$ is an $N \times P$ matrix consisting of the corresponding fraction of each endmember.

By using LMM, the spatial sampled data Y_1 can be described as $A_1 S E$. Since the special structure of matrix A_1 , $A_1 S$ has the same structure as S . Therefore, the spectral unmixing algorithm can be performed on the compressed sampled data to extract endmembers and abundance. Before endmember extraction, the number of endmembers in the hyperspectral images should be estimated. Hyperspectral signal identification by the minimum error (HySime)^[13] is employed to estimate the endmember number, p , and the vertex

component analysis (VCA)^[14] algorithm is used to extract the endmembers from the spatial sampled data, Y_1 . The VCA to obtain the endmember matrix is as follow.

The p endmember spectra are first extracted from Y_1 and stored in endmember matrix E . Then an intermediate vector v is chosen such that no object is orthogonal to it. Next, all objects are projected into v and the first endmember corresponding to the maximum of the projection. The succeeding endmembers are iteratively projected to a subspace orthogonal to the span of the endmembers already determined. This is done until the p endmembers are found.

Since both Y_1 and Y_2 are obtained from the same scenario, the endmembers extracted from Y_1 can also be regarded as the endmembers of Y_2 . Thus, the spectral sampled data Y_2 can be expressed by introducing a new matrix, B , as follows:

$$Y_2 = SB \quad (7)$$

where $B = EA_2^T$ is the compressed endmembers matrix. Since E and A_2 are known, B is known. Our goal is to find the abundance matrix, S , from spectral sampled data Y_2 . Note that the p value presented in a given scenario is usually much smaller than the number of L values; however, the p value may be smaller than the J value when SR_2 is large. In this case, the least squares method can be used to estimate S from the spectral sampled data, Y_2 , because B is a full-rank matrix. Once we obtain endmember matrix E and abundance matrix S , the original hyperspectral image can be reconstructed from the sampled data according to Eq.(6).

3 Experimental results and discussion

The proposed algorithm was evaluated on both raw and calibrated datasets collected in 2005 by an Airborne Visible Infrared Imaging Spectrometer (AVIRIS) sensor, which was pioneered by the Jet Propulsion Laboratory of the US National Aeronautics and Space Administration. All sequences comprised

224 bands recorded at different wavelengths in the range of 380 to 2 500 nm, with a spectral resolution of 10 nm. The tested datasets were represented in 16 bits, and each image had 512 lines, 224 bands, and 512 pixels per line.

3.1 Reconstruct performance

We demonstrate the reconstruct performance of proposed compressed sensing algorithm. For comparison purposes, we also show results obtained with state-of-the-art CPPCA^[5]. We let the total sampling rate vary from 0.1 to 0.5. Figure 4 shows the average SNR(signal-to-noise ratio) of the recovered hyperspectral imagery(aviris_sc0.raw and aviris_sc3.raw) with different sampling rates. We can see that the reconstruct average SNR ascends with the increase of the oversampling rate. The reconstruct performance of proposed algorithm outperforms the CPPCA. CPPCA lacks stability when the number of measurements is bellow the true signal subspace. However, the proposed algorithm still keeps a higher reconstruct precision when the sampling rate is less than 0.2.

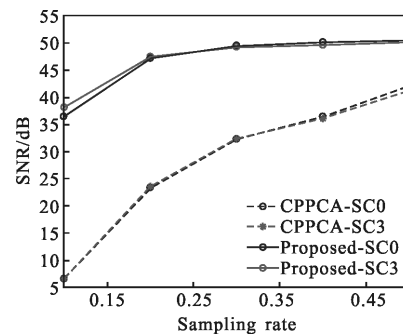


Fig.4 SNR curves of different methods on AVIRIS raw data

3.2 Compression performance

In this study, we used the bit per pixel per band (bpppb) and the SNR to evaluate the compression performance. The block size $s \times s$ was selected as 32×32 for the proposed algorithm. The final bpppb was determined by the spatial sampling rate, spectral sampling rate, and lossless compression method. We compared the results of the proposed algorithm with JPEG2000, DCT-JPEG2000 and DWT-JPEG2000 using a large range of bitrates. Note that JPEG2000 is

a well-known compression standard that is primarily used for still image compression. DCT-JPEG2000 is a widely employed lossy compression algorithm that removes the spectral correlation using the discrete cosine transform (DCT) followed by a spatial wavelet transform with full post-compression rate-distortion optimization (PCRD-opt). DWT-JPEG2000 is similar to DCT-JPEG2000, with the only difference being the spectral de-correlation, which removes the spectral correlation by using the discrete wavelet transform (DWT). The compression results on the AVIRIS raw image through various algorithms are shown in Fig.5. As shown in Fig.5, although JPEG2000 has a perfect rate-distortion performance for the still image, its rate distortion performance for the hyperspectral image is not satisfactory on account of the lack of spectral decorrelation. DWT-JPEG2000 provides the best rate

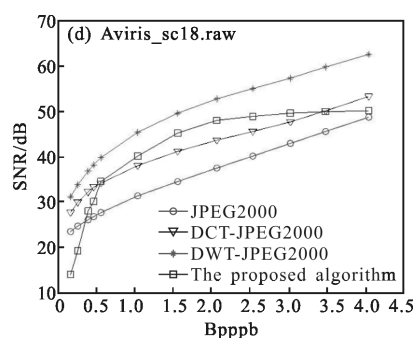
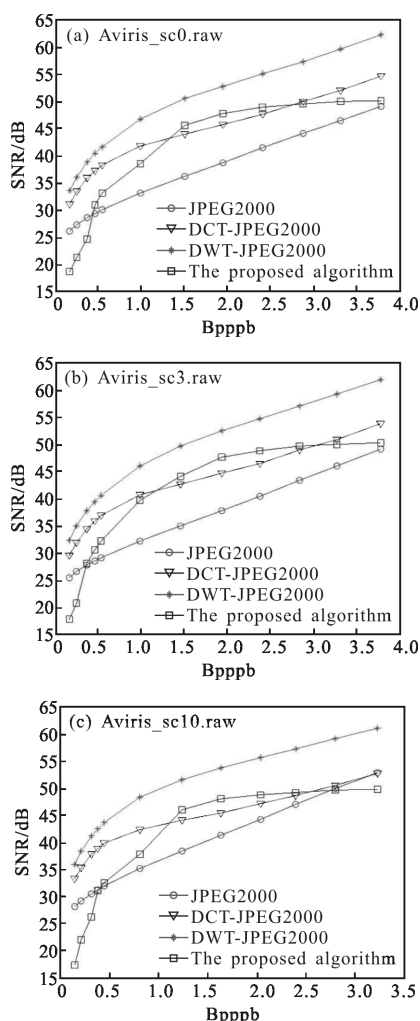


Fig.7 Comparison of rate distortion performance for AVIRIS raw data

distortion performance owing to its high performance in spectral decorrelation. The performance of DCT-JPEG2000 is lower than that of DWT-JPEG2000 because DCT is less efficient than DWT for spectral decorrelation. With regard to the proposed algorithm, the performance at low bitrates was the worst, even lower than that of JPEG2000, which was because of the inherent limitation of the prediction-based lossy compression algorithm. However, this disadvantage can be negligible at high bitrates. At the middle and high bitrates, the performance of the proposed algorithm was higher than that of JPEG2000. Even in a partial range of bitrates, the proposed algorithm outperformed DCT-JPEG2000. However, because the coding technique of the proposed algorithm is simple and much less powerful than that of PCRD-opt, the performance of the proposed algorithm was less than that of DWT-JPEG2000. In sum, the proposed algorithm showed better performance than JPEG2000, and even better performance than DCT-JPEG2000 at some bitrates, whereas it showed a lower performance than DWT-JPEG2000.

3.3 Complexity

In terms of complexity, the proposed algorithm mainly employs spatio-spectral hybrid sampling and linear prediction to realize hyperspectral image compression, which provides lower encoder complexity than the transform-based algorithm. Since the sampling can be directly realized by optical devices, this process does not cost any computing. As for the prediction process, the proposed algorithm requires approximately 6 additions and 3 multiplications per pixel. To evaluate the complexity of the proposed



algorithm, the runtime was employed to compare the complexity of each algorithm, including both encoder and decoder complexity. A comparison of complexity for various algorithms is reported in Tab.1. Although DWT–JPEG2000 shows the best performance, its complexity is the highest. DCT–JPEG2000 has modest complexity, which is lower than that of DWT–JPEG2000 and higher than that of JPEG2000; however, there is a performance gap between DCT and DWT for spectral decorrelation. The proposed algorithm shows better performance than JPEG2000; however, its encoder complexity is lower.

Tab.1 Comparison of complexity of various algorithms

Algorithm	Encoder/ms	Decoder/ms
JPEG2000	61	23
DCT–JPEG2000	126	30
DWT–JPEG2000	138	50
Proposed algorithm	39	15

4 Conclusion

Hyperspectral imaging has an immense data volume; thus, traditional compression algorithms have difficulty satisfying the related requirements of onboard storage and transmission. In this paper, we proposed a CS–based lossy compression technique for hyperspectral images using spectral unmixing. The CS technique can effectively reduce the data volume by using a certain measurement matrix, which significantly reduces the encoder complexity. The spatio-spectral hybrid sampling is performed on the original hyperspectral image at first. Then, the correlation of the sampled data is studied, and spectral linear prediction is employed to remove the spectral correlation of sampled data followed by JPEG–LS lossless compression. At the decoder, spectral unmixing is performed on the decoded data to recover the original hyperspectral image. Experimental results showed that proposed algorithm has competitive compression performance compared with the transform-based compression algorithm. Moreover, the proposed algorithm has low computational complexity of both the encoder and decoder, which is suitable for the efficient

compression of the onboard hyperspectral image.

References:

- [1] Penna B, Tillo T, Magli E, et al. Transform coding techniques for lossy hyperspectral data compression[J]. *IEEE Transactions on Geoscience and Remote Sensing*, 2007, 45(5): 1408–1421.
- [2] Blanes I, Serra-Sagrista J. Pairwise orthogonal transform for spectral image coding[J]. *IEEE Transactions on Geoscience and Remote Sensing*, 2011, 49(3): 961–972.
- [3] Nian Y J, Liu Y, Ye Z. Pairwise KLT–based compression for multispectral images [J]. *Sensing and Imaging*, 2016, 17(1): 1–15.
- [4] Donoho D L. Compressed sensing[J]. *IEEE Transactions on Information Theory*, 2006, 52(4): 1289–1306.
- [5] Fowler J E. Compressive-projection principal component analysis[J]. *IEEE Transactions on Image Processing*, 2009, 18(10): 2230–2242.
- [6] Jia Y B, Feng Y, Wang Z L. Reconstructing hyperspectral images from compressive sensors via exploiting multiple priors[J]. *Spectroscopy Letters*, 2015, 48(1): 22–26.
- [7] Chen C, Li W, Tramel E W, et al. Reconstruction of hyperspectral imagery from random projections using multihypothesis prediction [J]. *IEEE Transactions on Geoscience and Remote Sensing*, 2014, 52(1): 365–374.
- [8] Li C B, Sun T, Kelly K F, et al. A compressive sensing and unmixing scheme for hyperspectral data processing[J]. *IEEE Transactions on Image Processing*, 2012, 21(3): 1200–1210.
- [9] Zhang L, Wei W, Zhang Y, et al. Locally similar sparsity-based hyperspectral compressive sensing using unmixing[J]. *IEEE Transactions on Computational Imaging*, 2016, 2(2): 86–100.
- [10] Zhang L, Wei W, Tian C N. Exploring structured sparsity by a reweighted laplace prior for hyperspectral compressive sensing [J]. *IEEE Transactions on Image Processing*, 2016, 25(10): 4974–4988.
- [11] Wang Z L, Feng Y, Jia Y B. Spatio-spectral hybrid compressive sensing of hyperspectral imagery [J]. *Remote Sensing Letters*, 2015, 6(3): 199–208.
- [12] Huo C F, Zhang R, Yin D. Compression technique for compressed sensing hyperspectral images [J]. *International Journal of Remote Sensing*, 2012, 33(5): 1586–1604.
- [13] Dias J M B, Nascimento J M P. Hyperspectral subspace identification [J]. *IEEE Transactions on Geoscience and Remote Sensing*, 2008, 46(8): 2435–2445.
- [14] Nascimento J M P, Dias J M B. Vertex component analysis: a fast algorithm to unmix hyperspectral data [J]. *IEEE Transactions on Geoscience and Remote Sensing*, 2005, 43(4): 898–910.